Supplement of

Aerosol light absorption from attenuation measurements of PTFE-membrane filter samples: implications for particulate matter monitoring networks

Apoorva Pandey[1], Nishit J. Shetty[1], and Rajan K. Chakrabarty[1,2]
[1]Center for Aerosol Science and Engineering, Department of Energy, Environmental and Chemical Engineering, Washington University in St. Louis, St. Louis, MO 63130, USA
[2]McDonnell Center for the Space Sciences, Washington University in St. Louis, St. Louis, MO 63130, USA

S1. Experimental methods

Fuel types and combustion conditions, with corresponding single scattering albedo (SSA) values and absorption Ångström exponents (AÅE), are listed in Table S1. Burn protocols for the three combustion phases were as follows:

1) Peat was smoldered using a heating plate at a temperature of 200□ C. Other biomass types were smoldered by first establishing flaming (for 1-2 min) by igniting the fuel with a lighter and then starving the flame by covering the fuel container. While the biomass was flaming, the chamber exhaust was left open; the exhaust was closed once the flames were extinguished. The sample line between the chamber and mixing volume was connected 5 min after closing the exhaust.
2) To isolate the flaming phase, the biomass was ignited with a lighter and the chamber exhaust was closed. We monitored the flame visually from outside the combustion chamber, closing off the sample line between the chamber and the mixing volume once the flames were out.
3) For mixed phase sampling, flaming was established following the procedure above and emissions were continuously pulled into the mixing volume even after the flames were extinguished.

Some biomass types like Ponderosa pine and Douglas fir did not sustain smoldering combustion and were only sampled in flaming and mixed conditions. Other types like dung and Lodgepole pine were found to not sustain a flame. Kerosene was burned using a wick lamp. Intrinsic optical properties from the combustion of certain biomass types varied from burn to burn for the same combustion protocol. For such cases, the ranges of observed properties are given in the table below. During each burn, a steady state (10-40 min long) was established within which the absorption and scattering coefficients were nearly constant.

Table S1: Number of burns conducted and filter samples collected for each fuel type and combustion phase in this study. Intrinsic optical properties of emissions from each study condition are also given.

Fuel	Combustion phase	SSA 375 nm	SSA 405 nm	SSA 532 nm	AÅE 375-532 nm	Number of burns	Number of filter samples
Dung	smoldering	0.86	0.95	0.98	6.1-6.6	6	7
Peat	smoldering	0.92	0.97	0.99	4.8-6.8	2	3
Sage	smoldering	0.75-0.87	0.86-0.93	0.93-0.97	2.8-5.3	4	14
	mixed	0.56-0.77	0.69-0.84	0.71-0.87	1.5-2.3	3	7
	flaming	0.43-0.65	0.62-0.69	0.69-0.77	0.9-1.4	2	5
Grass	smoldering	0.74	0.87	0.94	3.2-4.7	3	7
	flaming	0.76	0.81	0.85	1.7	1	3
Lodgepole pine	smoldering	0.84	0.93	0.97	4.2	2	3
Ponderosa pine	mixed	0.61-0.84	0.74-0.91	0.76-0.95	1.2-3.0	4	9
	Flaming	0.56	0.65	0.65	0.7	1	2
Douglas fir	Mixed	0.82	0.89	0.93	2.7	1	2
	Flaming	0.60	0.70	0.71	0.9	1	3
Hardwood pellets	Mixed	0.80-0.87	0.92-0.95	0.95-0.98	4.1-6.1	1	3
Kerosene	Flaming	0.27	0.30	0.31	0.7-1.1	3	7

S2. Two-stream model

Consider the layer of filter in which sampled particles are embedded to be a one-dimensional uniform medium with an optical thickness τ_0, a single scattering albedo $\omega<1$ and a scattering asymmetry parameter g. Now, consider a 'forward' direction: at any point in the medium the energy intensity propagating in this direction is given by I_f. Conversely, the backward propagation intensity is I_b.

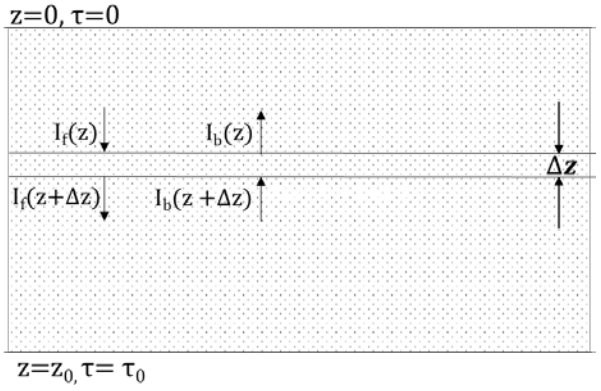

Figure S1: Transmission and reflection of radiation through a one-dimensional, uniformly multiple-scattering medium.

Energy conservation in the medium can be written as[1]:

$$\frac{d(I_f - I_b)}{d\tau} = -(1-\omega_0)(I_f + I_b) \quad \text{(S1a)}$$

$$\frac{d(I_f + I_b)}{d\tau} = -(1-\omega_0 g))(I_f - I_b) \quad \text{(S1b)}$$

The general solution of the above equations has the following form:

$$(I_f - I_b) = p_1 \exp(-K\tau) + p_2 \exp(K\tau) \quad \text{(S2a)}$$

$$(I_f + I_b) = q_1 \exp(-K\tau) + q_2 \exp(K\tau) \quad \text{(S2b)}$$

where $K = \sqrt{(1-\omega_0)(1-\omega_0 g)}$

Assume that the medium is (1) illuminated from the top: $I_f(\tau = 0) = I_0$ and (2) does not reflect at the opposite edge: $I_b(\tau = \tau_0) = 0$. Reflectance R_l and transmittance T_l of the medium are respectively defined as: $I_b(\tau = 0) = R_l$ and $I_f(\tau = \tau_0) = T_l$. With these boundary conditions, the constants p_1, p_2, q_1 and q_2 can be estimated. Then the quantities of interest, R_l and T_l, are given by[2]:

$$R_l = \frac{\omega_0(1-g)\, sinh(K\tau_0)}{[2K - \omega_0(1-g)\, sinh(K\tau_0) + 2K\, cosh(K\tau_0)]} \quad \text{(S3a)}$$

$$T_l = \frac{2}{[2K - \omega_0(1-g)\, sinh(K\tau_0) + 2K\, cosh(K\tau_0)]} \quad \text{(S3b)}$$

Note that in the manuscript the subscript *l* is used in the equations above to denote the properties of a composite aerosol-filter layer. τ_0 denotes the total optical depth of the layer:

$$\tau_0 = \tau_{e,l} = \tau_{e,f} + \tau_{a,s} + \tau_{sc,s} \quad \text{(S4)}$$

Subscripts *e, a* and *sc* denote extinction, absorption and scattering optical depths. The second subscript *f* corresponds to the portion of the filter that was penetrated by the aerosol, while *s* represents the aerosol sample. Eq. (4) can be rewritten as:

$$\tau_{e,l} = \chi\tau_{e,F} + \tau_{a,s}\left(\frac{1+\omega_s}{1-\omega_s}\right) \quad \text{(S5)}$$

where χ is the penetration depth of the aerosols in the filter (assumed 0.1 in this study). A two-layer schematic of the filter with a given aerosol penetration depth is showed in Fig. S2. The optical depth of the filter in the first layer is proportional to the penetration depth and the optical depth of a blank filter, $\tau_{e.F.}$ In eq. S5, ω_s is the single scattering albedo of the deposited aerosols. The single scattering albedo and asymmetry parameter of this composite layer are given by:

$$\omega_0 = \frac{\tau_{a,s}\left(\frac{\omega_s}{1-\omega_s}\right) + \chi\tau_{e,F}}{\tau_{a,s}\left(\frac{1+\omega_s}{1-\omega_s}\right) + \chi\tau_{e,F}} \quad \text{(S6)}$$

$$g = \frac{g_s \times \tau_{a,s}\left(\frac{\omega_s}{1-\omega_s}\right) + g_F \times \chi\tau_{e,F}}{\tau_{a,s}\left(\frac{\omega_s}{1-\omega_s}\right) + \chi\tau_{e,F}} \quad \text{(S7)}$$

The respective asymmetry parameters of the particles and filter are denoted by g_s and g_F. In this study, was g_s fixed at 0.6 (based on Martins et al.[3], Reid et al.[4]).

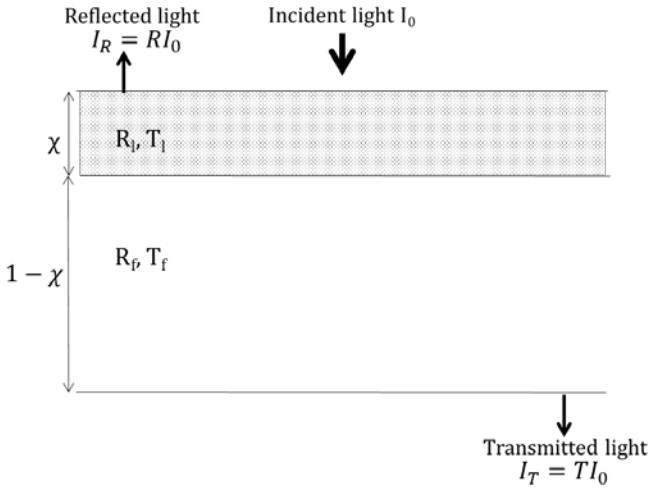

Figure S2: Two-layer model of a filter sample consisting of an aerosol laden layer 'l' and a pristine layer 'f'.

For the pristine portion of the filter (no aerosol embedded, therefore single scattering albedo is unity), the solution to Eq.s (S1a) and (S1b) is greatly simplified. The reflectance (*R2*) and transmittance (*T2*) of this layer is given by:

$$R_f = \frac{(1-\chi)\tau_F^*}{1+(1-\chi)\tau_F^*} \quad \text{(S8a)}$$

$$T_f = \frac{1}{1+(1-\chi)\tau_F^*} \quad \text{(S8b)}$$

where $\tau_F^* = \left(1 - g_F\right)\tau_F$ is estimated from the measurements of transmittance and reflectance through blank filters. Since a blank filter is non-absorbing, Eq.s (S8a) and (S8b) can be applied to it, setting χ as zero (i.e. no loading). Measured transmittance through 20 blank PTFE membrane filters for wavelengths ranging 350-550 nm was 0.7±0.02, this yield the value of τ^*_F:

$$\tau_F^* = \frac{1}{T_{blank}} - 1 = 0.43 \quad \text{(S9)}$$

It can be shown that all calculations in equations S3a through S8b require only τ^*_F and not τ_F and g_F. Therefore, any non-zero value can be assumed for τ_F and g_F can be calculated such that the value of τ^*_F is satisfied. With these filter properties (τ_F and g_F), and assumed aerosol penetration depth χ and asymmetry parameter g_s, R_l, R_f, T_l and T_f were calculated for a range of aerosol properties ($\tau_{a,s}$ and ω_s). Then, overall filter transmittance and reflectance were estimated by performing an energy balance[5]:

$$T = \frac{T_l T_f}{1-R_l R_f} \quad \text{(S10A)}$$

$$R = R_l + \frac{T_l^2 R_f}{1-R_l R_f} \quad \text{(S10B)}$$

S3. Filter correction factor *C*

Fig. S3 shows the filter correction factor *C* plotted against filter optical loading (attenuation) and the aerosol single scattering albedo. As the correction factor was calculated by dividing the absorption optical depth of the deposited aerosols by the attenuation through the corresponding filter sample, uncertainties in the correction factor contain experimental errors from both measurements. This combined error, as well as the mathematical nature of the relationship between absorption optical depth and attenuation, leads to difficulty in fitting a curve to the data in Fig. S3A. No correlation was found between the correction factor and attenuation datasets.

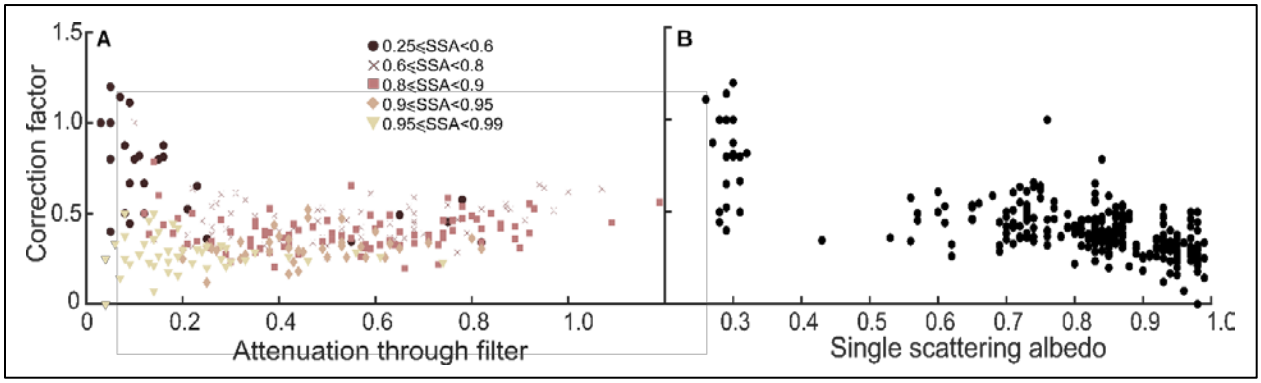

Figure S3: Correction factor *C* (ratio of absorption to attenuation) as a function of A) attenuation through the filter and B) single scattering albedo of the deposited particles.

S4. Application of correction equation to IMPROVE data

The Interagency Monitoring of Protected Visual Environments (IMPROVE) network routinely collects samples of fine particulate matter on Teflon, quartz and nylon filter substrates. The Teflon filter samples are analyzed for transmittance (*T*) and reflectance (*R*) using a Hybrid Integrating Plate and Sphere (HIPS) method. Attenuation is estimated using:

$$ATN = ln(\frac{1-R}{T}) \quad \text{(S11)}$$

Then, a filter-based absorption coefficient is inferred:

$$Fabs = ATN \times \frac{1}{L} \quad \text{(S12)}$$

Here, L represents the length of air column sampled and is calculated from the sample area, volumetric flow rate through the filters and the sampling duration. For the IMPROVE network, L is fixed at 93 km.[6]

Carbon fraction analysis is conducted on quartz filter samples using the IMPROVE thermo-optical reflectance (TOR) protocol. The non-refractory carbon fractions, minus the pyrolyzed organic content, are reported as EC.

We downloaded Fabs values at 633 nm and EC mass concentration data for all 223 sites for the year 2010, from the online IMPROVE repository (http://vista.cira.colostate.edu/Improve/improve-data/) on 06/05/2018. The sampling frequency was one sample every 3 days. After removing invalid data (displayed as -999 in the download), there remained 18313 points in the dataset. Of these, the points

corresponding to EC concentrations smaller than 0.01 (the lowest 3% of all data) were removed from analysis. Using Eq. (S12), ATN values were calculated from *Fabs*, and were corrected using the empirical relationship provided on the manuscript:

$$ATN_{cor} = 0.48\ (ATN)^{1.32} \quad \text{(S13)}$$

Then, a corresponding corrected absorption coefficient was calculated ($Fabs_{cor} = ATN_{cor} \times \frac{1}{L}$) using Eq. (S12). The relationship between the filter-based absorption coefficients, before and after applying the above correction, and EC mass concentrations is shown in Fig. S6. Linear regression analysis shows an improvement in the R^2 values and a reduction in the slope for corrected absorption coefficients. The slope of the lines represents a site- and time-average MAC value for EC, neglecting the contribution to light absorption from organic carbon or iron aerosols.

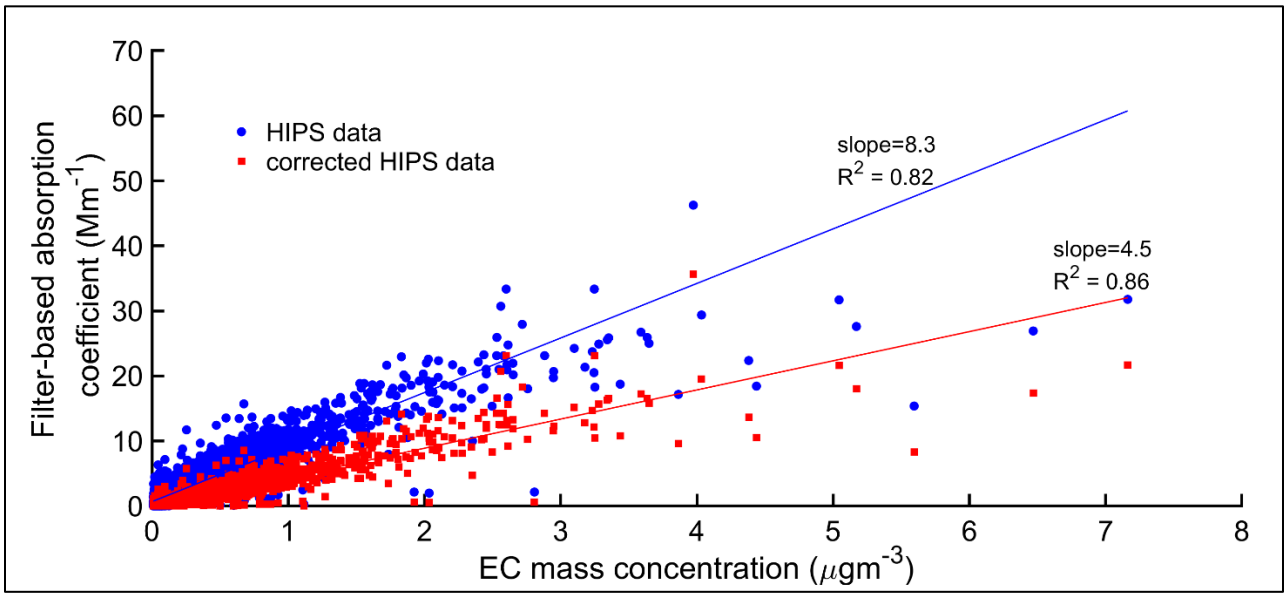

Figure S4: Filter-based absorption coefficients measured using the HIPS system from IMPROVE Teflon samples as functions of EC mass concentrations measured using collocated quartz filters. The absorption coefficients were also converted to attenuation values and corrected.

References

1. Bohren, C. F., Multiple scattering of light and some of its observable consequences. *Am. J. Phys* **1987,** *55*, (6), 524-533.
2. Arnott, W. P.; Hamasha, K.; Moosmüller, H.; Sheridan, P. J.; Ogren, J. A., Towards aerosol light-absorption measurements with a 7-wavelength aethalometer: Evaluation with a photoacoustic instrument and 3-wavelength nephelometer. *Aerosol Sci. Technol.* **2005,** *39*, (1), 17-29.
3. Martins, J. V.; Artaxo, P.; Liousse, C.; Reid, J. S.; Hobbs, P. V.; Kaufman, Y. J., Effects of black carbon content, particle size, and mixing on light absorption by aerosols from biomass burning in Brazil. *Journal of Geophysical Research: Atmospheres* **1998,** *103*, (D24), 32041-32050.
4. Reid, J.; Koppmann, R.; Eck, T.; Eleuterio, D., A review of biomass burning emissions part II: intensive physical properties of biomass burning particles. *Atmos. Chem. Phys.* **2005,** *5*, (3), 799-825.

5. Gorbunov, B.; Hamilton, R.; Hitzenberger, R., Modeling radiative transfer by aerosol particles on a filter. *Aerosol Science & Technology* **2002,** *36*, (2), 123-135.
6. White, W. H.; Trzepla, K.; Hyslop, N. P.; Schichtel, B. A., A critical review of filter transmittance measurements for aerosol light absorption, and de novo calibration for a decade of monitoring on PTFE membranes. *Aerosol Sci. Technol.* **2016,** *50*, (9), 984-1002.